IEEE Access
Multidisciplinary | Rapid Review | Open Access Journal

Received August 9, 2021, accepted August 21, 2021, date of publication August 25, 2021, date of current version August 31, 2021.

Digital Object Identifier 10.1109/ACCESS.2021.3107955

Energy-Efficient Index Modulation With In-Phase/Quadrature Format in the Generalized Fading Channel

MENGYI WANG[1], ZHIHUI CHEN[2], AND ZHENXING CHEN[3]
[1]School of Electronic Information, Wuhan University, Wuhan 430072, China
[2]School of Artificial Intelligence, North China University of Science and Technology, Tangshan 063009, China
[3]School of Mechanical Engineering and Electronic Information, China University of Geosciences, Wuhan 430074, China

Corresponding author: Zhenxing Chen (Chenzx@cug.edu.cn)

This work was supported by the Natural Science Foundation of Hubei, China, under Grant 2020CFB563.

ABSTRACT Dual-mode (DM) or multi-mode (MM) index modulation (IM) techniques with the in-phase/quadrature (IQ) format have been investigated for improving the performance of the orthogonal frequency division multiplexing with IM (OFDM-IM) system in the frequency-selective Rayleigh fading channel. However, all subcarriers in these schemes must be activated so that the energy efficiency (EE) of the system inevitably decreases. In this paper, we propose a novel modulation scheme named quadrature tri-mode index modulation (QTM-IM) technique to achieve a trade-off between the spectral efficiency (SE) and EE. The proposed QTM-IM can also be flexibly extended into multi-mode form called MM with enhanced IQ (MM-EIQ). The multi-mode M-ary pulse amplitude modulation (PAM) constellations containing the origin point are designed to map the information bits into the active subcarriers. On the other hand, the theoretical analysis of IM-based schemes over the Rician fading channel has been conducted since most previous papers only considered the Rayleigh fading channel. At the receiver, three kinds of detectors with different algorithm complexities are employed for signal demodulation. Finally, the computer simulation results demonstrate the enhancement of the proposed schemes. More specially, (i) QTM-IM achieves 4dB signal-to-noise ratio (SNR) gain at the BER level of 10^{-5} compared with quadrature DM (QDM) scheme with the same SE in the Rician fading channel and (ii) MM-EIQ harvests 0.89 bits/s/Hz SE gain and almost doubles the EE compared with MM-IQ scheme without any SNR loss over the Rayleigh fading channel.

INDEX TERMS Index modulation (IM), orthogonal frequency division multiplexing (OFDM), multi-mode pulse amplitude modulation (PAM) constellation, spectral efficiency (SE), energy efficiency (EE), bit error rate (BER).

I. INTRODUCTION

Index modulation (IM), a novel modulation technique, has been considered for its application to the fifth-generation (5G) wireless networks [1], [2], which can utilize the time slot [3], spreading codes [4], antenna index [5], and subcarrier index to implicitly transmit information bits without extra energy consumption [6], [7].

Recently, a promising IM technique known as spatial modulation (SM) has emerged which utilizes the spatial domain to transmit information bits besides the conventional signal constellations [7]. Therefore, the fundamental principle of SM is an extension of the two-dimensional constellation (e,g. quadrature amplitude modulation (QAM) and phase shift keying (PSK)) to a novel third dimension, which is spatial dimension. This new technique motivates the researchers to apply the SM principle to the subcarriers in an orthogonal frequency division multiplexing (OFDM) system. The first attempt is [8], where the subcarrier index modulation OFDM (SIM-OFDM) is proposed. In this scheme, the extra information is conveyed by the specific choice of the active subcarrier indices in an on-off keying (OOK) manner and these indices are determined by their corresponding majority bit-values of the OOK streams. However, this technique imposes a potential bit error propagation and results in the bursts of errors. In order to solve this issue, the enhanced

The associate editor coordinating the review of this manuscript and approving it for publication was Mehdi Hosseinzadeh.

SIM-OFDM (ESIM-OFDM) was introduced in [9], where only half of the subcarriers are modulated. Although this scheme improves the attainable error performance, the high order constellation are required for mapping to acquire the same spectral efficiency (SE) as the classical OFDM.

Combining IM and OFDM techniques, called OFDM with IM (OFDM-IM), is proposed in [10]. In the OFDM-IM system, all subcarriers are divided into several subblocks, and the coming information bits are transmitted not only by the constellation symbols but also by the indices of subcarriers in each subblock. The energy efficiency (EE) of OFDM-IM system is higher than that of the classical OFDM due to the inactive subcarriers with zero value are contained. Some important intrinsic properties such as the diversity order and achievable rate of IM-based OFDM systems are analysed in [11]. To enhance the throughput, the concept of OFDM-IM can also applied in the multiple-input multiple-output system [12] or the advanced terahertz wireless communication scene [13]. In order to increase the number of the index bits, a scheme named layered OFDM-IM (L-OFDM-IM) was proposed in [14], where the subcarriers in a subblock are partitioned into several layers and the activated subcarriers and their symbols are determined in each layer separately. In [15] and [16], two different interleaving techniques are also introduced in OFDM-IM to obtain the additional diversity gain and enhance the error performance of the system.

Designing the secondary constellation to modulate the ''inactive'' subcarriers is also an efficient approach to improve OFDM-IM performance. In [17], the dual-mode index modulation aided OFDM (DM-OFDM) is proposed to improve the achievable transmission rate of OFDM-IM in which only a part of subcarriers are activated for constellation symbol mapping. Besides the information bits carried by subcarrier indices, all subcarriers are modulated by two distinguishable constellations in DM-OFDM. The zero-padded tri-mode OFDM with IM (ZTM-OFDM-IM) is proposed in [18], where only a part of subcarriers are modulated by two different constellations while the inactive subcarriers are contained to improve EE compared with DM-OFDM. Moreover, the multiple-mode OFDM-IM (MM-OFDM-IM) is introduced in [19], where the multiple signal constellations are applied for symbol modulation and these different modes are used for additional index information transmission. In [20], a new modulation schemes called Q-ary MM-OFDM-IM (Q-MM-OFDM-IM) is proposed to further improve the proportion of the index bits compared with MM-OFDM-IM by using disjoint multi-mode constellations.

In order to achieve more possible realizations in an OFDM subblock, the generalized index modulation technique (GIM) is investigated. In the GIM technique, the number of the activated subcarriers or the subcarriers modulated by one selected signal constellation are no longer fixed, necessitating the appearance of OFDM-GIM [21], GDM-OFDM [22] and GMM-OFDM-IM [23].

On the other hand, each subcarrier maps a complex constellation symbol in the aforementioned schemes. However, the IM can be separately performed on the in-phase and quadrature (IQ) components, necessitating the appearance of OFDM with the IQ-IM (OFDM-IQ-IM) and doubling the number of index bits [24]. Similiarly, Quadrature DM-OFDM (QDM-OFDM) and MM-IQ-OFDM-IM have also been proposed in [25] and [19], respectively, aiming to improve the SE corresponding to the existing counterparts. The signal constellations for these IQ schemes are designed in [19]. A simple but effective technique named linear constellation precoding (LCP) can be employed in the IQ-IM-based schemes to achieve the diversity gain and ultra-reliable performance compared with the conventional OFDM-IQ-IM [26] and also applied in MM-OFDM-IM [27].

However, the EE of the multi-mode IQ-IM based schemes in [25] and [19] are low because all subcarriers are activated. Therefore, a new IQ-IM technique with higher EE and its corresponding constellation design are necessary to be investigated. On the other hand, the performance of most existing IM-based schemes are only studied over the Rayleigh fading channel. Hence, the theoretical and simulated performance over the general fading channel such as the frequency selective Rician fading channel is also necessary to be researched.

In this paper, we firstly propose a new modulation scheme called quadrature tri-mode OFDM with IM (QTM-OFDM-IM). In the proposed scheme, the IM process is independently executed on the in-phase and quadrature components, where the corresponding dual-mode pulse amplitude modulation (PAM) constellations are designed for constellation symbol mapping. In order to ensure the high EE, the inactive subcarrier with zero value must be contained in the in-phase and quadrature components. Then, the proposed QTM-IM can be flexibly extended into multi-mode form to make full use of possible index combinations and we name this new technique as MM with enhanced IQ (MM-EIQ). The overall comparison is conducted from the perspectives of the SE, EE and detection complexity. Unlike QDM-OFDM and MM-IQ-OFDM-IM, the origin point is considered in the designed PAM constellation. Any order and any mode constellation for the proposed scheme can be obtained by our straightforward design strategy. In terms of the theoretical analysis of the bit error rate (BER) performance, an expression with integral form are derived when the Rician fading is considered. At the receiver, three kinds of detectors based on the maximum-likelihood (ML) criterion or logarithm-likelihood-ratio (LLR) criterion are employed for signal demodulation. Finally, simulation results show that the proposed schemes harvest better error performance with improved SE and EE than other IM-based or IQ-IM-based schemes under the Rayleigh and Rician fading channels. In addition, the simulated BER curves of the proposed scheme are tightly limited by the theoretical upper bounds derived in this paper.

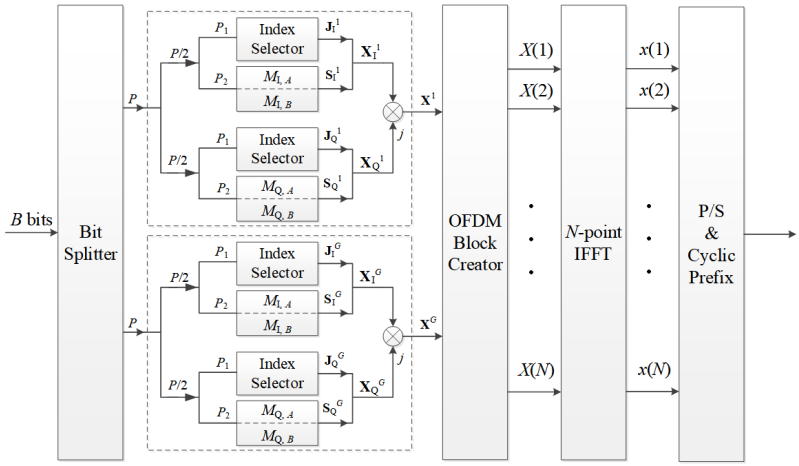

FIGURE 1. The structure of the proposed QTM-OFDM-IM transmitter.

The main contributions of this paper can be summarized as follows.

- A new IQ-IM technique named quadrature tri-mode index modulation is introduced, where the inactive subcarrier with zero value must be contained in the in-phase and quadrature components. Then, QTM-IM can be flexibly extended into MM-EIQ to exploit more index combinations. A quantitative comparison of the proposed and other existing schemes, in terms of the SE, EE and detection complexity, is conducted and the table shows that MM-EIQ harvests the best performance.
- The corresponding multi-mode PAM constellations are designed for the proposed schemes. Unlike QDM-OFDM and MM-IQ-OFDM-IM, the zero-value subcarriers are contained in the proposed schemes to ensure the high EE. Therefore, the distance between the symbol and the origin point must be considered. The simulation results show that the designed strategy is appropriate in terms of the BER performance.
- Both theoretical and simulated BER performance of the proposed schemes and other existing IM-based schemes under the frequency-selective Rician fading channel are investigated. An approximate equation of the well-known Q function with the integral form rather than the polynomial form (e.g. [10]) is employed to acquire the expression of the theoretical BER curve.

The rest of this paper is organized as follows. The system model and channel model are described in section II. Three kinds of detectors and a design method for the multi-mode PAM constellation are also introduced. Thereafter, the extension of QTM-IM to MM-EIQ is introduced in section III. Section IV analyses the SE, EE and detection complexity of the proposed schemes and gives the mathematical expression of the BER curve in the Rician and Rayleigh fading channels. The simulation result and discussion are shown in section V. Finally, section VI draws some conclusions.

II. THE PROPOSED QTM-OFDM-IM SYSTEM

A. SYSTEM MODEL AND CHANNEL MODEL

The structure of the proposed QTM-OFDM-IM transmitter is plotted in Fig. 1. We assume that the coming B information bits are split into G subblocks with the length of l by the bit splitter, and the number of bits in each subblock is P, that is $G = B/P = N/l$, where N is the number of subcarriers in an OFDM block.

More specifically, we focus on the gth ($1 \le g \le G$) subblock for the explanation of the proposed scheme. At first, each P information bits are equally divided into two bit streams. The IM process is separately performed on the in-phase and quadrature components in a subblock. For the in-phase component, the first P_1 as index bits are fed into the index selector to decide the activation pattern of subcarrier component. The active subcarrier indices can be expressed as $\mathbf{J}_{\mathrm{I}}^{g} = [\mathbf{J}_{\mathrm{I},A}^{g}, \mathbf{J}_{\mathrm{I},B}^{g}]$, where $\mathbf{J}_{\mathrm{I},A}^{g} = [J_{\mathrm{I},A}^{g}(1),\ldots,J_{\mathrm{I},A}^{g}(k_1)]$ and $\mathbf{J}_{\mathrm{I},B}^{g} = [J_{\mathrm{I},B}^{g}(1),\ldots,J_{\mathrm{I},B}^{g}(k_2)]$ whose elements belonging to $[1, l]$. k_1 and k_2 are the number of subcarriers modulated by two PAM constellation sets $\mathbf{M}_{\mathrm{I},A}$ and $\mathbf{M}_{\mathrm{I},B}$ ($\mathbf{M}_{\mathrm{I},A} \cap \mathbf{M}_{\mathrm{I},B} = \emptyset$), with the size of $\sqrt{N_A}$ and $\sqrt{N_B}$, respectively. Note that $\mathbf{M}_{\mathrm{I},A}$ and $\mathbf{M}_{\mathrm{I},B}$ are the in-phase component of QAM constellations with the sizes of N_A and N_B. In this paper, we assume that different constellations have the same size and use N_A to denote the order of all constellations. In order to ensure the high EE of the proposed scheme, we set that $k_1 + k_2 = k < l$, where k is the number of active subcarriers in the in-phase component of a subblock. The remaining P_2 bits are mapped into the active subcarriers using two distinguishable constellations. The active subcarriers set are $\mathbf{S}_{\mathrm{I}}^{g} = [\mathbf{S}_{\mathrm{I},A}^{g}, \mathbf{S}_{\mathrm{I},B}^{g}]$, where $\mathbf{S}_{\mathrm{I},A}^{g} = [S_{\mathrm{I},A}^{g}(1), \ldots, S_{\mathrm{I},A}^{g}(k_1)] \in \mathbf{M}_{\mathrm{I},A}$ and $\mathbf{S}_{\mathrm{I},B}^{g} = [S_{\mathrm{I},B}^{g}(1),\ldots,S_{\mathrm{I},B}^{g}(k_2)] \in \mathbf{M}_{\mathrm{I},B}$. This means that the active subcarriers related to $\mathbf{J}_{\mathrm{I},A}^{g}$ and $\mathbf{J}_{\mathrm{I},B}^{g}$ are modulated by $\mathbf{S}_{\mathrm{I},A}^{g}$ and $\mathbf{S}_{\mathrm{I},B}^{g}$, respectively. Therefore, the output of the in-phase component in the gth subblock is $\mathbf{X}_{\mathrm{I}}^{g} = [X_{\mathrm{I}}^{g}(1),\ldots,X_{\mathrm{I}}^{g}(l)]$ and $X_{\mathrm{I}}^{g}(\alpha) \in \{\mathbf{S}_{\mathrm{I},A}^{g}, \mathbf{S}_{\mathrm{I},B}^{g}, 0\}$, $1 \le \alpha \le l$. For the quadrature component, the same modulation process is conducted and

TABLE 1. The mapping rule of QTM-OFDM-IM with $(l, k_1, k_2) = (3, 1, 1)$.

$P_{1,\mathrm{I}}$	$P_{1,\mathrm{Q}}$	$\mathbf{J}_\mathrm{I}$	$\mathbf{J}_\mathrm{Q}$	$\mathbf{X} = \mathbf{X}_\mathrm{I} + j\mathbf{X}_\mathrm{Q}$	$P_{1,\mathrm{I}}$	$P_{1,\mathrm{Q}}$	$\mathbf{J}_\mathrm{I}$	$\mathbf{J}_\mathrm{Q}$	$\mathbf{X} = \mathbf{X}_\mathrm{I} + j\mathbf{X}_\mathrm{Q}$
00	00	[1,2]	[1,2]	$[S_{\mathrm{I},A} + jS_{\mathrm{Q},A}, S_{\mathrm{I},B} + jS_{\mathrm{Q},B}, 0]$	10	00	[2,3]	[1,2]	$[0 + jS_{\mathrm{Q},A}, S_{\mathrm{I},A} + jS_{\mathrm{Q},B}, S_{\mathrm{I},B}]$
00	01	[1,2]	[2,1]	$[S_{\mathrm{I},A} + jS_{\mathrm{Q},B}, S_{\mathrm{I},B} + jS_{\mathrm{Q},A}, 0]$	10	01	[2,3]	[2,1]	$[0 + jS_{\mathrm{Q},B}, S_{\mathrm{I},A} + Sj_{\mathrm{Q},A}, S_{\mathrm{I},B}]$
00	10	[1,2]	[2,3]	$[S_{\mathrm{I},A}, S_{\mathrm{I},B} + jS_{\mathrm{Q},A}, 0 + jS_{\mathrm{Q},B}]$	10	10	[2,3]	[2,3]	$[0, S_{\mathrm{I},A} + jS_{\mathrm{Q},A}, S_{\mathrm{I},B} + jS_{\mathrm{Q},B}]$
00	11	[1,2]	[3,2]	$[S_{\mathrm{I},A}, S_{\mathrm{I},B} + jS_{\mathrm{Q},B}, 0 + jS_{\mathrm{Q},A}]$	10	11	[2,3]	[3,2]	$[0, S_{\mathrm{I},A} + jS_{\mathrm{Q},B}, S_{\mathrm{I},B} + jS_{\mathrm{Q},A}]$
01	00	[2,1]	[1,2]	$[S_{\mathrm{I},B} + jS_{\mathrm{Q},A}, S_{\mathrm{I},A} + jS_{\mathrm{Q},B}, 0]$	11	00	[3,2]	[1,2]	$[0 + jS_{\mathrm{Q},A}, S_{\mathrm{I},B} + jS_{\mathrm{Q},B}, S_{\mathrm{I},A}]$
01	01	[2,1]	[2,1]	$[S_{\mathrm{I},B} + jS_{\mathrm{Q},B}, S_{\mathrm{I},A} + jS_{\mathrm{Q},A}, 0]$	11	01	[3,2]	[2,1]	$[0 + jS_{\mathrm{Q},B}, S_{\mathrm{I},B} + jS_{\mathrm{Q},A}, S_{\mathrm{I},A}]$
01	10	[2,1]	[2,3]	$[S_{\mathrm{I},B}, S_{\mathrm{I},A} + jS_{\mathrm{Q},A}, 0 + jS_{\mathrm{Q},B}]$	11	10	[3,2]	[2,3]	$[0, S_{\mathrm{I},B} + jS_{\mathrm{Q},A}, S_{\mathrm{I},A} + jS_{\mathrm{Q},B}]$
01	11	[2,1]	[3,2]	$[S_{\mathrm{I},B}, S_{\mathrm{I},A} + jS_{\mathrm{Q},B}, 0 + jS_{\mathrm{Q},A}]$	11	11	[3,2]	[3,2]	$[0, S_{\mathrm{I},B} + jS_{\mathrm{Q},B}, S_{\mathrm{I},A} + jS_{\mathrm{Q},A}]$

the output can be expressed as $\mathbf{X}_\mathrm{Q}^g = [X_\mathrm{Q}^g(1),\ldots,X_\mathrm{Q}^g(l)]$ and $X_\mathrm{Q}^g(\alpha) \in \{\mathbf{S}_{\mathrm{Q},A}^g, \mathbf{S}_{\mathrm{Q},B}^g, 0\}$. Combining the in-phase and quadrature components, the output signal of the gth subblock can be represented as $\mathbf{X}^g = \mathbf{X}_\mathrm{I}^g + j\mathbf{X}_\mathrm{Q}^g$. As an example, when (l, k_1, k_2) are set to (3, 1, 1), the mapping rule of the proposed QTM-OFDM-IM is shown in Table 1, where $P_1 = [P_{1,\mathrm{I}}, P_{1,\mathrm{Q}}]$, $\mathbf{J}_\mathrm{I}$ and $\mathbf{J}_\mathrm{Q}$ are the subcarrier activation patterns, respectively, of the IQ components and the index of the subblock g is omitted.

Remark: In order to make the proposed scheme be more flexible, the critical parameters such as k_1 and k_2 are not necessary identical in the in-phase and quadrature components because the demodulation procedure is independent (discussed in section II.B) for these two branches. This can be achieved by the definition of the mapping rule table at both the transmitter and receiver sides. However, we assume that the system parameters are the same in the IQ branches in this paper without loss of generality.

According to the proposed modulation scheme, the number of bits carried by an OFDM subblock can be calculated as

$$P = 2\left(\lfloor \log_2(C_l^k C_k^{k_1}) \rfloor + k \log_2(\sqrt{N_A})\right), \tag{1}$$

where C_l^k is binomial coefficient and $\lfloor . \rfloor$ denotes integer floor operator. Concatenating all G subblocks in the OFDM block creator, the OFDM signal in the frequency domain can be built. The transmitted OFDM signal in the time domain can be obtained by N-point inverse fast Fourier transform (IFFT). After the parallel-to-serial (P/S) conversion and appending the cyclic prefix (CP) with the length of L_{cp}, the generated OFDM signals are transmitted through a time-invariant fading channel shown in Fig. 2, where "TS" means transmitter side and "RS" means receiver side [28].

The channel can be modeled by its channel impulse response (CIR) $\mathbf{h}_\mathrm{T} = [h_\mathrm{T}(1), \ldots, h_\mathrm{T}(\nu)]^T$, where $(.)^T$ means transposition and $h_\mathrm{T}(u)$, $1 \le u \le \nu$, represents the complex Gaussian random variables. Assume that the number of propagation paths ν is smaller than L_{CP}. Given that N-point FFT operation has been performed on the zero-padded $\mathbf{h}_\mathrm{T}$, the resulting signal $\mathbf{H} = [H(1), \ldots, H(N)]^T$ is also a Gaussian vector with mean $\mathbf{H}_\mathrm{m} = [H_\mathrm{m}(1), \ldots, H_\mathrm{m}(N)]^T$ and covariance matrix $C_H = E\{(H - H_\mathrm{m})(H - H_\mathrm{m})^H\}$,

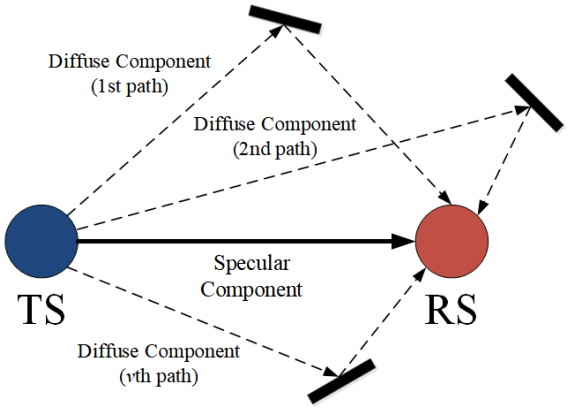

FIGURE 2. The model of the time-invariant fading channel.

where $E\{.\}$ denotes the expectation operation and $(.)^H$ is Hermitian transposition.

Furthermore, the mean of the channel vector elements in the frequency domain $H(i)$, $1 \le i \le N$, determines the type of the channel. When $H_\mathrm{m}(i) = 0$, the absolute value of $H(i)$ has the Rayleigh distribution because of the diffuse propagation (see dotted line in Fig. 2). On the contrary, it is the Rician fading channel when $H(i)$ has a nonzero mean due to the specular propagation (see real line in Fig. 2).

Hence, the channel vector can be rewritten as

$$H = H_\mathrm{m} + H_\mathrm{d} = \sqrt{\frac{Z}{Z+1}} H_\mathrm{mn} + \sqrt{\frac{1}{Z+1}} H_\mathrm{dn}, \tag{2}$$

where $\mathbf{H}_\mathrm{m}$ represents the specular component, $\mathbf{H}_\mathrm{d}$ denotes the diffuse component and the constant Z-factor is defined as the power ratio of two components. Assume that all subcarriers share the identical Z-value. After the normalization, the elements in $\mathbf{H}_\mathrm{mn}$ are equal to one and the elements in $\mathbf{H}_\mathrm{dn}$ follow the distribution of $\mathcal{CN}(0,1)$.

At the receiver, the output frequency-domain OFDM signal of the gth subblock after N-point FFT can be expressed as

$$Y^g = \mathrm{diag}(X^g)H^g + Z^g,\ 1 \le g \le G, \tag{3}$$

where $\mathrm{diag}(X^g)$ denotes a diagonal matrix with the elements of X^g, H^g denotes the CIR coefficients of the fading channel

in the frequency domain and Z^g represents the additive Gaussian white noise (AWGN) with the variance N_0 in the frequency domain. Then, we will give three kinds of detectors based on the ML and LLR criterions with different detection complexities in the next subsection.

B. DETECTOR

1) ML DETECTOR

A ML detector is exploited at the receiver, where all possible subblock realizations are considered to recover the index bits and constellation symbols. The detection process in detail can be formulated as

$$[\hat{J}^g, \hat{X}^g] = \arg \min_{J^g, X^g} \|Y^g - \text{diag}(X^g)H^g\|^2. \quad (4)$$

In terms of the number of complex multiplication, the computational complexity in (4) is $O(4^{p_1}N_A^k)$ per subblock.

2) EQUIVALENT ML DETECTOR

According to [24], we can conclude that the in-phase and quadrature components are mutually independent in the detection procedure. Hence, we choose the in-phase part as the illustrative case. After the zero-forcing equalizer, the received OFDM signal in the gth subblock can be given as $Y_{\text{e}}^g(\alpha) = Y^g(\alpha)/H^g(\alpha)$ and we have

$$[\hat{J}_{\text{I}}^g, \hat{X}_{\text{I}}^g] = \arg \min_{J_{\text{I}}^g, X_{\text{I}}^g} \sum_{i=1}^{n} |H^g(i)|^2 |\text{Re}(Y_e^g(i)) - X_{\text{I}}^g(i)|^2, \quad (5)$$

where Re(.) represents the operation of real part. It can be observed that the equivalent ML detector decouple the in-phase and quadrature components by a zero-forcing equalizer. Therefore, the detection complexity for this detector is on the order of $O(2^{(p_1+1)}(\sqrt{N_A})^k)$ which is much lower than the ML detector. However, it is also unpractical when p_1 and k become large because of its exponentially increasing complexity.

3) TWO-STAGE LLR DETECTOR

In order to alleviate the complexity issue, a two-stage LLR detector is employed for the proposed QTM-OFDM-IM. The demodulation processes are identical for the in-phase and quadrature components. For the in-phase component, the LLR values can be calculated as

$$\gamma_\alpha = \ln \left(\frac{\sum_{j=1}^{N_{\text{I},A}+N_{\text{I},B}} P(X_{\text{I}}^g(\alpha) = S_{\text{I},C}(j) | \text{Re}(Y_{\text{e}}^g(\alpha)))}{P(X_{\text{I}}^g(\alpha) = 0 | \text{Re}(Y_{\text{e}}^g(\alpha)))} \right), \quad (6)$$

where $N_{\text{I},A} = \sqrt{N_A}$ and $N_{\text{I},B} = \sqrt{N_B}$. $S_{\text{I},C}(j)$ is jth element of $M_{\text{I},C} = M_{\text{I},A} \cup M_{\text{I},B}$. Thus, the k largest LLR values decide the active subcarriers J_{I}^g. Considering Bayes' formula, (6) can be rewritten as:

$$\gamma_\alpha = \ln(\frac{k_1}{N_{\text{I},A} + N_{\text{I},B}}) + \frac{|H^g(\alpha)|^2 \text{Re}(Y_{\text{e}}^g(\alpha))^2}{N_0} + \ln(\sum_{j=1}^{N_{\text{I},A}+N_{\text{I},B}} \exp(\frac{|H^g(\alpha)|^2 |\text{Re}(Y_{\text{e}}^g(\alpha)) - S_{\text{I},C}(j)|^2}{-N_0}), \quad (7)$$

In order to avoid the potential numerical overflow, the Jocobian logarithm [10] is applied to calculate the third item in (7). Therefore, the value of γ_α can be calculated by iterative Algorithm 1, where $F = k_1/(N_{\text{I},A}+N_{\text{I},B})$. As shown in Algorithm 1, the received signal and channel coefficient in the frequency domain, PAM constellation sets and other system parameters are required to obtain the corresponding LLR value of each subcarrier.

Algorithm 1 Iterative LLR Calculation

Require: Received signal $Y_{\text{e}}^g(\alpha)$, CIR coefficient $H^g(\alpha)$, constellation sets $M_{\text{I},A}$ and $M_{\text{I},B}$, and system parameters $(l, k, N_{\text{I},A}, N_{\text{I},B})$.

Ensure: γ_α is the LLR value of αth subcarrier

```
Δ1 ⇐ −(1/N0) | H^g(α) |^2 | Re(Y_e^g(α)) − S_{I,C}(j) |^2;
i ⇐ 2;
while i ≤ N_{I,A} + N_{I,B} do
    T1 ⇐ −(1/N0) | H^g(α) |^2 | Re(Y_e^g(α)) − S_{I,C}(j) |^2;
    T2 ⇐ max{Δ1, T1}+ln(1+exp(-|Δ1 − T1|));
    Δ1 ⇐ T2;
    i ⇐ i + 1;
end while
γα ⇐ ln(F) − (1/N0) | H^g(α) |^2 Re(Y_e^g(α))^2 + Δ1;
return γα.
```

Based on the output of the first stage, the second stage of the LLR detector is conducted to determine whether the active subcarriers modulated by $\mathbf{M}_{\text{I},A}$ or $\mathbf{M}_{\text{I},B}$, which can be calculated as

$$\gamma_\alpha^* = \ln \left(\frac{\sum_{j=1}^{N_{\text{I},A}} P(X_{\text{I}}^g(\alpha) = S_{\text{I},A}(j) | \text{Re}(Y_{\text{e}}^g(\alpha)))}{\sum_{j=1}^{N_{\text{I},B}} P(X_{\text{I}}^g(\alpha) = S_{\text{I},B}(j) | \text{Re}(Y_{\text{e}}^g(\alpha)))} \right), \quad (8)$$

where $S_{\text{I},A}(j)$ and $S_{\text{I},B}(j)$ are the jth element, respectively, of the constellation sets $\mathbf{M}_{\text{I},A}$ and $\mathbf{M}_{\text{I},B}$. By means of (8), we can decide that the subcarrier is more possibly modulated by $M_{\text{I},A}$ if the corresponding γ_α^* is larger. According to the decided indices, the index bits and constellation symbols can be recovered by hard detection. Considering Bayes' formula, (8) can be rewritten as:

$$\gamma_\alpha^* = \ln(\frac{N_{\text{I},B}k_1}{N_{\text{I},A}k_2}) + \ln(\sum_{j=1}^{N_{\text{I},A}} \exp(-\frac{|\text{Re}(Y_{\text{e}}^g(\alpha)) - S_{\text{I},A}(j)|^2}{(1/|H^g(\alpha)|)^2 N_0}) + \ln(\sum_{j=1}^{N_{\text{I},B}} \exp(\frac{|H^g(\alpha)|^2 |\text{Re}(Y_{\text{e}}^g(\alpha)) - S_{\text{I},B}(j)|^2}{-N_0}). \quad (9)$$

The computational complexity of the LLR detection in terms of complex multiplication is $O(2l(N_{\text{I},A}+N_{\text{I},B}))$ which is significantly lower than the ML and equivalent ML detectors. Based on the discussion about the signal demodulation, we will give the design principles of the constellation in next subsection.

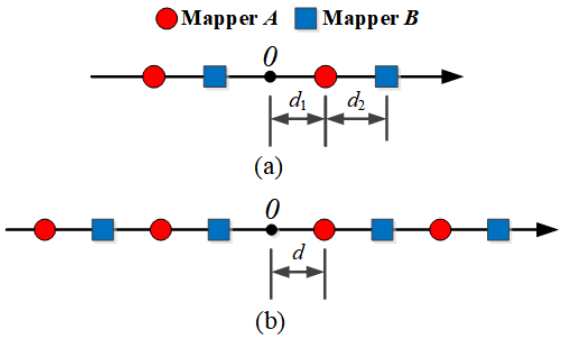

FIGURE 3. Two designed dual-mode PAM constellations for the proposed QTM-OFDM-IM. (a)$N_{I,A}$=$N_{I,B}$=2 (b)$N_{I,A}$=$N_{I,B}$=4.

C. CONSTELLATION DESIGN

The constellation design is crucial to the proposed QTM-OFDM-IM scheme. Two designed dual-mode PAM constellations for the proposed scheme are shown in Fig. 3. According to the system model in section II.A and Fig. 3(a), the error performance of the index bit is determined by

(i) the minimum distance between the symbols and the origin point, which is d_1 and

(ii) the minimum distance between two symbols from two different constellations, which is d_2.

On the other hand, when the receiver correctly demodulate all the index bits, the error performance of the symbol bits is determined by the minimum distance between two signal points of one selected constellation, which is $(2d_1 + d_2)$.

Therefore, we divide the PAM symbols into two subsets by assigning alternate points to each subset, as shown in Fig. 3(a). Unlike the constellation exploited in the QDM-OFDM and MM-IQ-OFDM-IM, the origin point should be considered because the inactive subcarriers exist in the proposed scheme. The remaining procedure is to determine the optimum value of d_1 and d_2 under the unit power constraint which can be formulated as

$$\begin{aligned} &max\ d_1, d_2, 2d_1 + d_2 \\ &s.t.\ d_1^2 + (d_1 + d_2)^2 = 2. \end{aligned} \tag{10}$$

Thereafter, we will give the objective function in designing the constellation in terms of the minimization of BER and also propose a simple method to design it.

The probability of the misjudgement from one subblock realization to another one in the index modulation scheme can be expressed as [19]

$$\sum_{X_{\mathrm{I}}^g, X_{\mathrm{I,e}}^g} \left[\prod_{\alpha=1}^{l} \left(1 + \frac{1}{2N_0} |X_{\mathrm{I}}^g(\alpha) - X_{\mathrm{I,e}}^g(\alpha)|^2 \right) \right]^{-1} + \sum_{X_{\mathrm{I}}^g, X_{\mathrm{I,e}}^g} \left[3 \prod_{\alpha=1}^{l} \left(1 + \frac{2}{3N_0} |X_{\mathrm{I}}^g(\alpha) - X_{\mathrm{I,e}}^g(\alpha)|^2 \right) \right]^{-1}, \tag{11}$$

where the parameters are defined in section IV.B.

According to (11) and [19], the BER in the high SNR region is proportional to the following (12), which is written as a function of $d_a = 2 * d_1 + d_2$, $d_i = \min(d_1, d_2)$ and $\rho = 1/N_0$,

$$\mathrm{BER} \propto \varepsilon_a \left[\left(1 + \frac{d_a^2}{2} \rho \right)^{-1} + \left(1 + \frac{2d_a^2}{3} \rho \right)^{-1} \right] + \varepsilon_i o(\rho^{-1}), \tag{12}$$

where ε_a and ε_i are the number of bits, respectively, corresponding to d_a and d_i and the higher order term $o(\rho^{-1})$ can be expressed as a function of d_i (because the index bits are more effective than symbols bits in the high SNR region [10]).

Therefore, the objective function of (10) can be formulated as

$$\begin{aligned} \mathrm{OF}(d_a, d_i) = \varepsilon_a &\left[\left(1 + \frac{d_a^2}{2} \rho \right)^{-1} + \left(1 + \frac{2d_a^2}{3} \rho \right)^{-1} \right] \\ &+ \varepsilon_i \left[\left(1 + \frac{d_i^2}{2} \rho \right)^{-2} + \left(1 + \frac{2d_i^2}{3} \rho \right)^{-2} \right]. \end{aligned} \tag{13}$$

It should be noted that the optimal d_a and d_i should have the minimum value of (13). However, the optimal values of d_1 and d_2 need to be determined separately with different system parameters which is too inconvenient. On the other hand, if we see the origin point as a special signal point in our scheme, we could uniformly place all signal points on the axis by setting $d_1 = d_2$. Given that the average power of symbols is normalized to unit, the coordinate values of the designed constellation can be computed as

$$\sum_{n=1}^{\sqrt{N_A}} (nd)^2 = \sqrt{N_A}. \tag{14}$$

Although the parameter d in (14) maybe not optimal, the method is flexible for the high-order constellation design. Besides, the simulation results in section IV demonstrate that the error performance of the proposed scheme with the designed constellation is better than that of the existing schemes. When $N_{\mathrm{I},A} = N_{\mathrm{I},B} = 2$, $d_1 = d_2 = 0.6325$, that is $M_{\mathrm{I},A} = \{-0.6325, 1.2649\}$ and $M_{\mathrm{I},B} = \{-1.2649, 0.6325\}$. In the case of $N_{\mathrm{I},A} = N_{\mathrm{I},B} = 4$, the designed PAM constellation is shown in Fig. 3 (b) with $M_{\mathrm{I},A} = \{-4d, -2d, d, 3d\}$ and $M_{\mathrm{I},B} = \{-3d, -d, 2d, 4d\}$, where d calculated by (14) is 0.3651.

From above description about the system model and detection procedure, we can flexibly extend the QTM-OFDM-IM into the multi-mode form aiming to generate more index combinations.

III. EXTENSION TO MULTI-MODE FORM

The system model in section II.A can be extended into multiple-mode form. In the extended system, the index selector should firstly choose k active subcarriers and every subcarrier is modulated by an unique signal constellation.

TABLE 2. The Comparison of SE, EE and Detection Complexity.

Scheme	$N_A = 4$					$N_A = 16$				
	SE	EE	ML	E-ML	LLR	SE	EE	ML	E-ML	LLR
IM(4,2)	1.33	2.66	2^6		16	2.22	4.44	2^{10}		64
IQ-IM(4,2)	1.78	3.56	2^8	2^5	16	2.67	5.33	2^6	2^7	32
DM(4,2)	2.22	2.22	2^6		32	4	4	2^{18}		128
QDM(4,2)	2.67	2.67	2^{12}	2^7	32	4.44	4.44	2^{20}	2^{11}	64
ZTM(4,2,1)	2	2.67	2^9		64	3.33	4.44	2^{15}		256
QTM(4,2,1)	2.67	3.56	2^{12}	2^7	64	4	5.33	2^{10}	2^{10}	128
MM(4,N_A)	2.67	2.67	2^{12}		100	4.44	4.44	2^{20}		464
MM-IQ(4,$\sqrt{N_A}$)	3.56	3.56	2^{16}	2^9	116	5.33	5.33	2^{24}	2^{13}	232
MM-EIQ(4,3,$\sqrt{N_A}$)	3.11	4.15	2^{14}	2^8	64	4.44	5.92	2^{13}	2^{11}	128

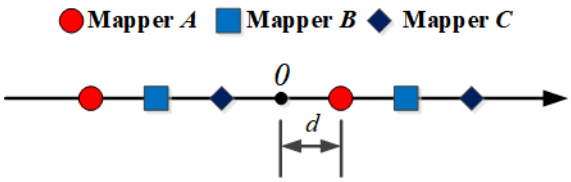

FIGURE 4. Multi-mode PAM constellation for the proposed MM-EIQ-OFDM-IM.

Therefore, there are a total of k different constellations and $C_n^k k!$ kinds of index combinations are generated. Therefore, the SE of the proposed scheme can be calculated as (15).

$$P = 2\left(\lfloor \log_2(C_n^k k!) \rfloor + k \log_2(\sqrt{N_A})\right). \tag{15}$$

As an example, we assume that $n = 3, k = 3, \sqrt{N_A} = 2$ and three different signal constellations are employed. The corresponding constellation is illustrated in Fig. 4 according to the design strategy in section II.C. It is interesting to discover that this scheme can be regarded as an enhanced MM-IQ scheme (MM-EIQ) because the inactive subcarriers are contained and the EE are improved. Aiming to be fairly compared with MM-IQ-OFDM-IM, the number of active subcarriers should be equal to that of constellations in MM-EIQ-OFDM-IM which is different from QTM-OFDM-IM and QDM-OFDM.

Two novel schemes have been described in detail. For explicitly show the enhancement of our proposed schemes, the overall comparison and theoretical analysis of the BER are necessary which is conducted in the next section.

IV. PERFORMANCE ANALYSIS

A. COMPARISON OF SE, EE AND DETECTION COMPLEXITY

From [29], we defined the SE and EE, respectively, as (16) and (17):

$$\eta = B/(N + L_{\mathrm{CP}}) \quad \text{[bits/s/Hz]}, \tag{16}$$

$$\lambda = \eta/(k/l) \quad \text{[bits/Joule]}, \tag{17}$$

where the EE λ is defined as the ratio of SE per unit bandwidth and the average energy per subcarrier. The comparison of the SE, EE and detection complexity of the proposed scheme and other index modulation schemes are listed in Table 2, where the parameters are given in the beginning of Section V.

As shown in Table 2, the LLR detector significantly reduces the detection complexity compared with the ML detector and the equivalent ML (E-ML) detector, especially when the high-order constellation is employed. In terms of the LLR detector, the proposed QTM-OFDM-IM trebles and doubles the number of complex multiplication compared with OFDM-IQ-IM and QDM-OFDM, respectively, but achieve a trade-off between the SE and EE. It also can be observed that the detection complexity of MM-EIQ using LLR detector is lower than its two counterparts because fewer constellations are employed. In addition, the proposed MM-EIQ achieves the highest EE due to the index bits occupy the largest proportion compared to other schemes without energy consumption. According to [10], the higher EE leads to better BER performance in the high signal-to-noise ratio (SNR) region because of the improved error performance of index bits, which is more effective with high SNR values.

B. UPPER BOUND ON BIT ERROR PROBABILITY

The average bit error probability (ABEP) can be applied to acquire the upper bound for the BER performance of the OFDM system with IM technique when the ML detector is utilized [10]. Due to the in-phase and quadrature components in the proposed schemes are identical, we only present the analysis of in-phase component for brevity. The in-phase component of the gth OFDM subblock can be represented as $X_{\mathrm{I}}^g = \mathrm{diag}\{[X_{\mathrm{I}}^g(1), \ldots, X_{\mathrm{I}}^g(l)]^{\mathrm{T}}\}$ and the corresponding CIR coefficients are $H^g = [H^g(1), \ldots, H^g(l)]^{\mathrm{T}}$. Assume that X_{I}^g is erroneously detected as $X_{\mathrm{I,e}}^g$, the conditional PEP (CPEP) can be denoted as:

$$P(X_{\mathrm{I}}^g \to X_{\mathrm{I,e}}^g \mid H^g) = Q(\delta/2N_0), \tag{18}$$

where $Q(x)$ denotes the well-known Gaussian Q-function and $\delta = \|(X_{\mathrm{I}}^g - X_{\mathrm{I,e}}^g)H^g\|^2 = A^H A$ with $A = (X_{\mathrm{I}}^g - X_{\mathrm{I,e}}^g)H^g$. Note

that A is with mean $\mathbf{\Omega} = (X_{\mathrm{I}}^g - X_{\mathrm{I,e}}^g)H_{\mathrm{m}}^g$ and covariance matrix:

$$\begin{aligned} C_A &= E\left\{[(X_{\mathrm{I}}^g - X_{\mathrm{I,e}}^g)H_{\mathrm{m}}^g][(X_{\mathrm{I}}^g - X_{\mathrm{I,e}}^g)H_{\mathrm{m}}^g]^H\right\} \\ &= (X_{\mathrm{I}}^g - X_{\mathrm{I,e}}^g)C_H(X_{\mathrm{I}}^g - X_{\mathrm{I,e}}^g)^H. \end{aligned} \tag{19}$$

In order to obtain the expression of closed-form unconditional PEP (UPEP), the approximation of the Gaussian Q-function in (20) is applied.

$$Q(x) = \frac{1}{\pi}\int_0^{\frac{\pi}{2}} \exp(-\frac{x^2}{2\sin^2\theta})d\theta. \tag{20}$$

Using the probability density function (PDF) of the given A in [30],

$$f(A) = \frac{\pi^{-n}}{\det(C_A)}\exp(-(A-\mathbf{\Omega})^H C_A^{-1}(A-\mathbf{\Omega})), \tag{21}$$

and the UPEP can be calculated as (24).

$$\begin{aligned} &P(X_{\mathrm{I}}^g \to X_{\mathrm{I,e}}^g) \\ &= E_{H^g}\left\{\frac{1}{\pi}\int_0^{\frac{\pi}{2}} \exp(-\frac{(A^HA)}{q\sin^2\theta})d\theta\right\}, \end{aligned} \tag{22}$$

$$= \frac{1}{\pi}\int_A\int_0^{\frac{\pi}{2}} \exp\left(\frac{-qA^HA}{\sin^2\theta}\right)\frac{\mathrm{e}^{(-(A-\mathbf{\Omega})^H\mathbf{C}_A(A-\mathbf{\Omega}))}}{\pi^n\det(E\{AA^H\})}d\theta dA, \tag{23}$$

$$= \frac{1}{\pi}\int_0^{\frac{\pi}{2}} \frac{1}{\det\left(\frac{qC_A}{\sin^2\theta}+I_l\right)}\exp(\mathbf{\Omega}^H(C_A+\frac{\sin^2\theta}{q}I_l)\mathbf{\Omega})d\theta, \tag{24}$$

where $E_{H^g}\{.\}$ denotes the expectation operation with respect to H^g, q=$1/(4N_0)$ and I_l represents the identity matrix. It should be noted that (22) and (23) are related via the property of Hermitian and the mathematical fact that the proper complex Gaussian joint probability density function integrates to one. Unfortunately, the integration in (24) is too complex to obtain a closed-form expression. However, it can be easily computed by the numerical method.

In the case of Rayleigh fading channel ($\mathbf{\Omega}$=0), the expression of UPEP can be simplified as (25).

$$P(X_{\mathrm{I}}^g \to X_{\mathrm{I,e}}^g) = \frac{1}{\pi}\int_0^{\frac{\pi}{2}}\left[\det\left(\frac{qC_A}{\sin^2\theta}+I_l\right)\right]^{-1}d\theta. \tag{25}$$

Aiming to obtain a closed-form expression of (25), we apply the eigenvalue-decomposition on C_A with rank R and get the different eigenvalues λ_r ($1 \le r \le R$). Then, (25) can be revaluated as

$$\begin{aligned} &P(X_{\mathrm{I}}^g \to X_{\mathrm{I,e}}^g) \\ &= \frac{1}{\pi}\sum_{r=1}^{R}\prod_{i\neq r}(1-\frac{\lambda_i}{\lambda_r})^{-1}\int_0^{\frac{\pi}{2}}\left(\frac{\sin^2\theta}{\sin^2\theta+\frac{\lambda_r}{q}}\right)d\theta. \end{aligned} \tag{26}$$

Using the method in [31] to calculate the above integral, the expression in (26) can be rewritten as

$$P(X_{\mathrm{I}}^g \to X_{\mathrm{I,e}}^g) = \frac{1}{2}\sum_{r=1}^{R}\prod_{i\neq r}(1-\frac{\lambda_i}{\lambda_r})^{-1}\left(1-\sqrt{\frac{\lambda_r/q}{1+\lambda_r/q}}\right). \tag{27}$$

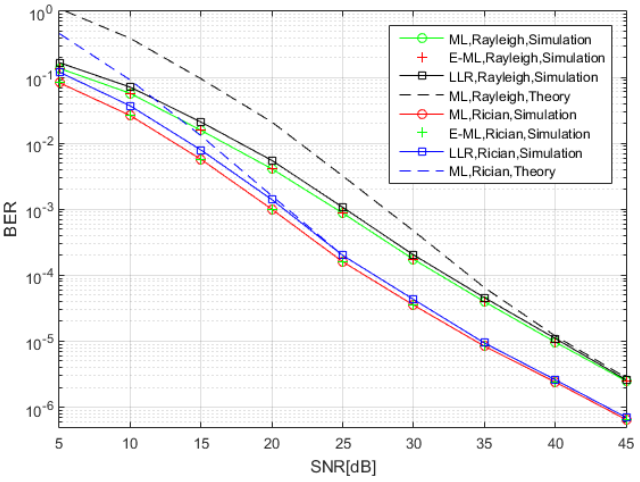

FIGURE 5. BER performance comparison of QTM-OFDM-IM using the ML, E-ML and LLR detectors under the Rayleigh and Rician fading channels.

Finally, based on the UPEP from (24) or (27), the ABEP of the proposed scheme can be represented as

$$P_b \approx \frac{1}{(P/2)2^{(P/2)}}\sum_{X_{\mathrm{I}}^g}\sum_{X_{\mathrm{I,e}}^g} P(X_{\mathrm{I}}^g \to X_{\mathrm{I,e}}^g)e(X_{\mathrm{I}}^g, X_{\mathrm{I,e}}^g), \tag{28}$$

where $e(X_{\mathrm{I}}^g, X_{\mathrm{I,e}}^g)$ represents the number of bit errors in the PEP event $P(X_{\mathrm{I}}^g \to X_{\mathrm{I,e}}^g)$.

In order to demonstrate the correctness of the theoretical analysis and superiority of the proposed schemes, computer simulations are carried out in the next section.

V. SIMULATION RESULTS AND DISCUSSIONS

Due to the fact that the proposed two schemes are IQ-IM-based, other existing IM-based and IQ-IM-based schemes are selected to conduct the comparison. In the simulation, the SNR per bit is defined as E_b/N_0, where E_b is the average energy per bit. The system parameters are set as follows: $N = 128$, $L_{\mathrm{CP}} = 16$, $\nu = 10$ and $Z = 2$. For brevity, we refer to "OFDM-(IQ)-IM (l, k)" as OFDM-(IQ)-IM system with k out of l subcarriers are activated in the IQ branches, "L-OFDM-IM (k, t, L)" as L-OFDM-IM system with 4 subcarriers in a subblock ($4 = t+k(L-1)$) for L layers, k out of t subcarriers are activated in each layer, "QDM-OFDM (l, k)" as QDM-OFDM system with k and $(l-k)$ subcarriers are modulated by two different constellations in the IQ branches. "QTM-OFDM-IM (l, k_1, k_2)" as QTM-OFDM-IM system with $(k_1 + k_2)$ out of l subcarriers are activated in the IQ branches, "MM-(IQ)-OFDM-IM (l, M)" as MM-(IQ)-OFDM-IM system with l subcarriers utilizing l different M-ary signal constellations in the IQ branches, "Q-MM-OFDM-IM(Q, l, M)" as Q-MM-OFDM-IM system utilizing Q disjoint M-ary constellation on l subcarriers in a subblock, "MM-EIQ-OFDM-IM (l, k, M)" as MM-EIQ-OFDM-IM system with k out of l subcarriers utilizing k different M-ary signal constellations in the IQ branches.

In Fig. 5, we compare the BER performance of the proposed QTM-OFDM-IM using the ML, Equivalent ML

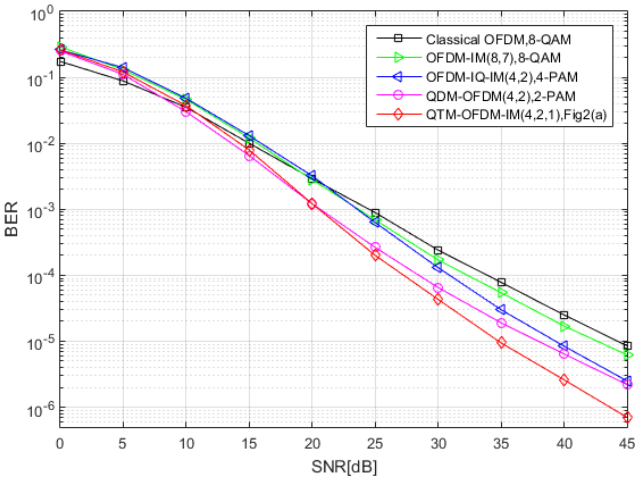

FIGURE 6. BER performance comparison among the classical OFDM, OFDM-IM, OFDM-IQ-IM, QDM-OFDM and QTM-OFDM-IM in the Rician fading channel (2.67bits/s/Hz).

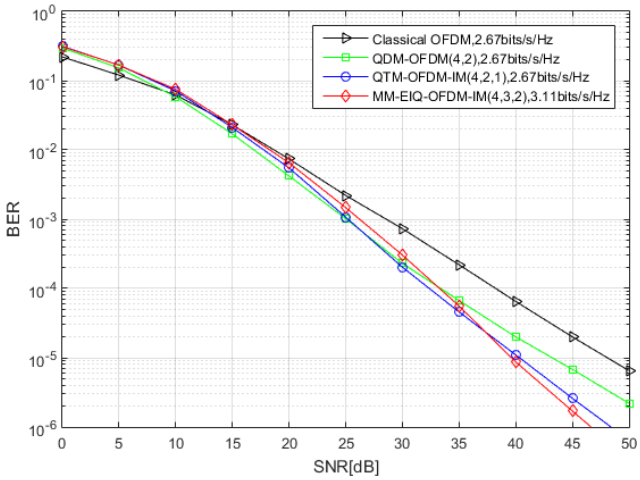

FIGURE 7. BER performance comparison among the classical OFDM, QDM-OFDM, QTM-OFDM-IM, MM-EIQ-OFDM-IM under the Rayleigh fading channel.

(E-ML) and LLR detectors under the Rayleigh and Rician fading channels when the constellation shown in Fig. 3(a) is employed. The SE of the system is set to 2.67bits/s/Hz. As shown in Fig. 5, the simulation results gradually match well with the theoretical upper bounds as SNR increases which demonstrates the accuracy of the theoretical analysis. It also can be seen that the PEP analysis in the Rician fading channel is more accurate than that of the Rayleigh fading channel because of the specular component. Due to the inherent problem of error propagation in the LLR detector, its performance is worse than the ML detector in the low SNR region. Fortunately, the performance loss is limited within 1dB. However, the LLR detector harvest near-optimal performance in the high SNR region because less error propagation happens. Additionally, the computational complexity for the LLR detector is significantly decreased to $O(64)$ compared with $O(4096)$ when the ML detector is used. It also can be found that the ML and E-ML detectors share the exactly identical performance.

Fig. 6 shows the BER performance of the classical OFDM with 8-QAM, OFDM-IM(8,7) with 8-QAM, OFDM-IQ-IM(4,2) with 4-PAM, QDM-OFDM(4,2) with 2-PAM and the proposed QTM-OFDM-IM with the designed constellation given in Fig. 3(a) under the Rician fading channel. All schemes share the same SE (2.67bits/s/Hz). We can see that OFDM-IM suffers from BER performance loss with low SNR values compared with the classical OFDM. This is because the misjudgement of index bits significantly degrades the performance of symbols bits. However, as SNR increases, OFDM-IM outperforms the classical OFDM. This can be explained by the fact that OFDM-IM provides an energy saving with 12.5% because of the inactive subcarriers. According to the diversity-order-theory in [10], the detector correctly detects all active indices with high SNR values and the error performance is only dominated by the decision error of constellation symbols. Therefore, a SNR gain of $20\log_{10}(8/7) \approx 1.2$dB should be found between OFDM-IM and the classical OFDM which corresponds to the result in Fig. 6. This interesting fact demonstrates the correctness of the diversity-order-theory in the Rician fading channel. In addition, the proposed scheme achieves the best BER performance when SNR is higher than 20dB due to its highest EE as discussed in section IV. A. More specifically, when the BER is at 10^{-5}, QTM-OFDM-IM harvests 3dB and 5dB, respectively, compared with OFDM-IQ-IM and QDM-OFDM. However, this advantage comes at a price of higher detection complexity.

Performance comparison among the classical OFDM with QPSK, QDM-OFDM(4,2) with 2-mode 2-PAM, QTM-OFDM-IM(4,2,1) with constellation given in Fig. 3(a) and MM-EIQ-OFDM-IM(4,3,2) with constellation shwon in Fig. 4 under the Rayleigh fading channel is given in Fig. 7. MM-IQ-OFDM-IM is not shown here because its lowest SE is 3.56 bits/s/Hz when $l = 4$. We can see that two proposed schemes achieve the best BER performance in the high SNR region. This can be understood that the proportion of index bits in MM-EIQ-OFDM-IM, which is 0.57, is higher than that in QTM-OFDM-IM (0.5) and QDM-OFDM (0.33). More specifically, the proposed QTM-OFDM-IM obtain about 3dB and 8dB performance gain over QDM-OFDM and the classical OFDM at the BER of 10^{-5}, respectively. Besides the advantage of BER performance, the SE of MM-EIQ-OFDM-IM is also significantly higher than that of QDM-OFDM and the classical OFDM.

In Fig. 8, BER performance comparison among the classical OFDM with 16-QAM, OFDM-IQ-IM(4,3) with 4-PAM, MM-IQ-OFDM-IM(4,2) with 4-mode 2-ary PAM constellation, and QTM-OFDM-IM(8,3,1) with the constellation shown in Fig. 3(b) under the Rayleigh fading channel is given. All schemes share the identical SE of 3.56bits/s/Hz. The SNR gain of QTM-OFDM-IM can reach about 2dB and 5dB compared with MM-IQ-OFDM-IM and OFDM-IQ-IM

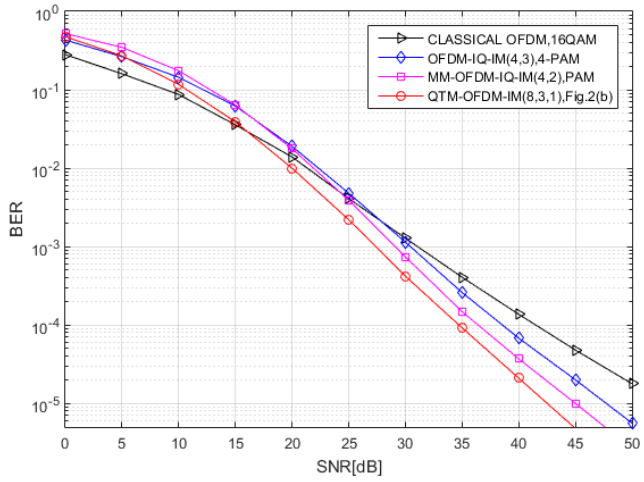

FIGURE 8. BER performance comparison among the classical OFDM, OFDM-IQ-IM, MM-IQ-OFDM-IM and QTM-OFDM-IM under the Rayleigh fading channel (3.56 bits/s/Hz).

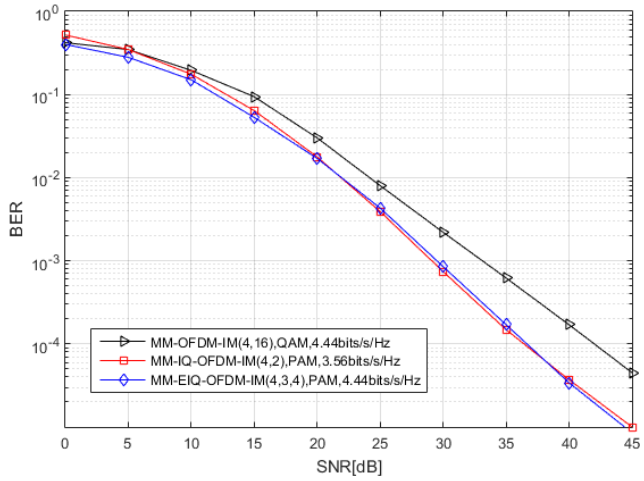

FIGURE 9. BER performance comparison among MM-OFDM-IM, MM-IQ-OFDM-IM and MM-EIQ-OFDM-IM under the Rayleigh fading channel.

at the BER of 10^{-5}, respectively. Although the proportion of the index bits in the proposed scheme and MM-IQ-OFDM-IM are identical (0.5), only half of subcarriers are activated in the former and harvests double EE compared with the latter. This indicates that the proposed QTM-OFDM-IM outperforms other modulation schemes with high order constellation.

It is difficult to make MM-IQ-OFDM-IM and MM-EIQ-OFDM-IM have the same EE. Therefore, we compare the two schemes with nearly identical BER performance in Fig. 9. The three-mode 4-ary PAM constellation can be obtained by design method in section II.C for the proposed MM-EIQ-OFDM-IM(4,3,4). In addition, MM-OFDM-IM(4,16) with 4-mode 16-ary QAM constellation is also given for comparison. As shown in Fig. 9, the proposed scheme harvest the significant SE gain (0.88bits/s/Hz) without the SNR loss when compared with MM-IQ-OFDM-IM. Besides,

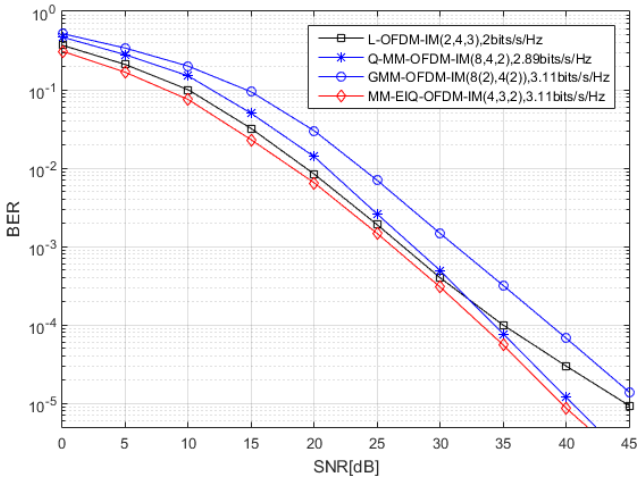

FIGURE 10. BER performance comparison among L-OFDM-IM, Q-MM-OFDM-IM, GMM-OFDM-IM and MM-EIQ-OFDM-IM under the Rayleigh fading channel.

the proposed scheme harvest 6dB SNR gain at the BER of 10^{-4} compared with MM-OFDM-IM with the identical SE.

Finally, we compare several advanced schemes which are proposed very recently in Fig. 10, including L-OFDM-IM with QPSK [14], Q-MM-OFDM-IM with 8-joint BPSK [20] and GMM-OFDM-IM [23] with MM-EIQ-OFDM-IM with the constellation shown in Fig. 4. GMM-OFDM-IM (8(2),4(2)) means 2 subcarriers modulated by 8-ary 2-mode PSK and 2 subcarriers by 2-mode 4-ary PSK in a subblock. As shown in the Fig. 10, MM-EIQ scheme achieves the best BER performance in the whole SNR region besides its significant SE improvement (1.11 bits/s/Hz) over L-OFDM-IM and 0.22 bits/s/Hz over Q-MM-OFDM-IM. More specially, at the BER level of 10^{-4}, the proposed scheme harvests 2dB and 6dB, respectively, over L-OFDM-IM and GMM-OFDM-IM.

VI. CONCLUSION AND FUTURE WORK

In this paper, a new IQ-IM-based modulation scheme named QTM-OFDM-IM is proposed. The in-phase/quadrature modulation format is exploited to enhance the SE of the system. At the same time, the inactive subcarriers are contained in each component to ensure the high EE compared with the existing systems. Then, this scheme is extended into multi-mode form to make full use of possible index combinations. The multi-mode M-ary PAM constellations considering the original point are designed. At the receiver, three kinds of detectors with different algorithm complexities are employed for signal demodulation. Simulation results show that the proposed schemes harvest better performance corresponding to other OFDM systems with IM or IQ-IM techniques under the Rayleigh and Rician fading channels.

The following points maybe considered as our future work: (i) because of the existence of inactive subcarrier, this energy-efficient multi-mode IQ-IM technique hardly achieves ultra-high SE. However, this issue can be solved by

further extending the proposed scheme into super-mode form to generate more index combinations, which is introduced in [32] very recently and (ii) the performance of the proposed scheme with channel coding techniques such as LCP in [26] and [27] and low-density parity-check coding (LDPC).

REFERENCES

[1] E. Basar, "Index modulation techniques for 5G wireless networks," *IEEE Commun. Mag.*, vol. 54, no. 7, pp. 168–175, Jul. 2016.
[2] E. Basar, M. Wen, R. Mesleh, M. Di Renzo, Y. Xiao, and H. Haas, "Index modulation techniques for next-generation wireless networks," *IEEE Access*, vol. 5, pp. 16693–16746, 2017.
[3] S. Lu, I. A. Hemadeh, M. El-Hajjar, and L. Hanzo, "Compressed-sensing-aided space-time frequency index modulation," *IEEE Trans. Veh. Technol.*, vol. 67, no. 7, pp. 6259–6271, Jul. 2018.
[4] G. Kaddoum, Y. Nijsure, and T. Hung, "Generalized code index modulation technique for high-data-rate communication systems," *IEEE Trans. Veh. Technol.*, vol. 65, no. 9, pp. 7000–7009, Sep. 2016.
[5] P. Yang, M. Di Renzo, Y. Xiao, S. Li, and L. Hanzo, "Design guidelines for spatial modulation," *IEEE Commun. Surveys Tuts.*, vol. 17, no. 1, pp. 6–26, 1st Quart., 2015.
[6] T. Mao, Q. Wang, Z. Wang, and S. Chen, "Novel index modulation techniques: A survey," *IEEE Commun. Surveys Tuts.*, vol. 21, no. 1, pp. 315–348, 1st Quart., 2019.
[7] Q. Li, M. Wen, B. Clerckx, S. Mumtaz, A. Al-Dulaimi, and R. Q. Hu, "Subcarrier index modulation for future wireless networks: Principles, applications, and challenges," *IEEE Wireless Commun.*, vol. 27, no. 3, pp. 118–125, Jun. 2020.
[8] R. Abu-Alhiga and H. Haas, "Subcarrier-index modulation OFDM," in *Proc. IEEE 20th Int. Symp. Pers., Indoor Mobile Radio Commun.*, Tokyo, Japan, Sep. 2009, pp. 177–181.
[9] D. Tsonev, S. Sinanovic, and H. Haas, "Enhanced subcarrier index modulation (SIM) OFDM," in *Proc. IEEE GLOBECOM Workshops*, Houston, TX, USA, Dec. 2011, pp. 728–732.
[10] E. Başar, U. Aygölü, E. Panayırcı, and H. V. Poor, "Orthogonal frequency division multiplexing with index modulation," *IEEE Trans. Signal Process.*, vol. 61, no. 22, pp. 5536–5549, Nov. 2013.
[11] M. Wen, X. Cheng, M. Ma, B. Jiao, and H. V. Poor, "On the achievable rate of OFDM with index modulation," *IEEE Trans. Signal Process.*, vol. 64, no. 8, pp. 1919–1932, Apr. 2016.
[12] E. Basar, "Multiple-input multiple-output OFDM with index modulation," *IEEE Signal Process. Lett.*, vol. 22, no. 12, pp. 2259–2263, Dec. 2015.
[13] T. Mao and Z. Wang, "Terahertz wireless communications with flexible index modulation aided pilot design," *IEEE J. Sel. Areas Commun.*, vol. 39, no. 6, pp. 1651–1662, Jun. 2021.
[14] J. Li, S. Dang, M. Wen, X.-Q. Jiang, Y. Peng, and H. Hai, "Layered orthogonal frequency division multiplexing with index modulation," *IEEE Syst. J.*, vol. 13, no. 4, pp. 3793–3802, Dec. 2019.
[15] E. Basar, "OFDM with index modulation using coordinate interleaving," *IEEE Wireless Commun. Lett.*, vol. 4, no. 4, pp. 381–384, Aug. 2015.
[16] Y. Liu, F. Ji, H. Yu, F. Chen, D. Wan, and B. Zheng, "Enhanced coordinate interleaved OFDM with index modulation," *IEEE Access*, vol. 5, pp. 27504–27513, 2017.
[17] T. Mao, Z. Wang, Q. Wang, S. Chen, and L. Hanzo, "Dual-mode index modulation aided OFDM," *IEEE Access*, vol. 5, pp. 50–60, Feb. 2017.
[18] T. Mao, Q. Wang, J. Quan, and Z. Wang, "Zero-padded orthogonal frequency division multiplexing with index modulation using multiple constellation alphabets," *IEEE Access*, vol. 5, pp. 21168–21178, Oct. 2017.
[19] M. Wen, E. Basar, Q. Li, B. Zheng, and M. Zhang, "Multiple-mode orthogonal frequency division multiplexing with index modulation," *IEEE Trans. Commun.*, vol. 65, no. 9, pp. 3892–3906, Sep. 2017.
[20] F. Yarkin and J. P. Coon, "Q-ary multi-mode OFDM with index modulation," *IEEE Wireless Commun. Lett.*, vol. 9, no. 7, pp. 1110–1114, Jul. 2020.
[21] R. Fan, Y. J. Yu, and Y. L. Guan, "Generalization of orthogonal frequency division multiplexing with index modulation," *IEEE Trans. Wireless Commun.*, vol. 14, no. 10, pp. 5350–5359, Oct. 2015.
[22] T. Mao, Q. Wang, and Z. Wang, "Generalized dual-mode index modulation aided OFDM," *IEEE Commun. Lett.*, vol. 21, no. 4, pp. 761–764, Apr. 2017.
[23] M. Wen, Q. Li, E. Basar, and W. Zhang, "Generalized multiple-mode OFDM with index modulation," *IEEE Trans. Wireless Commun.*, vol. 17, no. 10, pp. 6531–6543, Oct. 2018.
[24] B. Zheng, F. Chen, M. Wen, F. Ji, H. Yu, and Y. Liu, "Low complexity ML detector and performance analysis for OFDM with in-phase/quadrature index modulation," *IEEE Commun. Lett.*, vol. 19, no. 11, pp. 1893–1896, Nov. 2015.
[25] A. Bouhlel, S. Ikki, and A. Sakly, "Quadrature dual mode index modulation," *IEEE Wireless Commun. Lett.*, vol. 7, no. 4, pp. 542–545, Aug. 2018.
[26] M. Wen, B. Ye, E. Basar, Q. Li, and F. Ji, "Enhanced orthogonal frequency division multiplexing with index modulation," *IEEE Trans. Wireless Commun.*, vol. 16, no. 7, pp. 4786–4801, Jul. 2017.
[27] Q. Li, M. Wen, E. Basar, H. V. Poor, B. Zheng, and F. Chen, "Diversity enhancing multiple-mode OFDM with index modulation," *IEEE Trans. Commun.*, vol. 66, no. 8, pp. 3653–3666, Aug. 2018.
[28] J. Proakis, *Digital Communications*, 2nd ed. New York, NY, USA: McGraw-Hill, 1989.
[29] J. Joung, C. K. Ho, and S. Sun, "Spectral efficiency and energy efficiency of OFDM systems: Impact of power amplifiers and countermeasures," *IEEE J. Sel. Areas Commun.*, vol. 32, no. 2, pp. 208–220, Feb. 2014.
[30] V. V. Veeravalli, "On performance analysis for signaling on correlated fading channels," *IEEE Trans. Commun.*, vol. 49, no. 11, pp. 1879–1883, Nov. 2001.
[31] M.-S. Alouini and A. J. Goldsmith, "A unified approach for calculating error rates of linearly modulated signals over generalized fading channels," *IEEE Trans. Commun.*, vol. 47, no. 9, pp. 1324–1334, Sep. 1999.
[32] A. T. Dogukan and E. Basar, "Super-mode OFDM with index modulation," *IEEE Trans. Wireless Commun.*, vol. 19, no. 11, pp. 7353–7362, Nov. 2020.

MENGYI WANG received the B.S. degree in electronic and information engineering from China University of Geosciences, Wuhan, China, in 2020. He is currently pursuing the M.S. degree in circuits and systems with Wuhan University, Wuhan.

His current research interests include orthogonal frequency division multiplexing, index modulation, and array signal processing.

ZHIHUI CHEN received the B.S. degree in computer science and technology from Hebei Institute of Technology, Tangshan, China, in 2003, and the M.S. degrees from Beijing University of Technology, China, in 2009. She is currently an Assistant Professor with the School of Artificial Intelligence, North China University of Science and Technology, Tangshan.

Her research interests include intelligent signal processing and wireless communication.

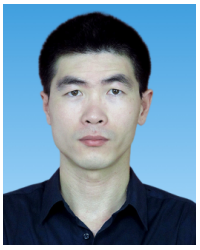

ZHENXING CHEN received the B.S. degree in electronic information engineering from the University of Science and Technology, LiaoNing, Anshan, China, in 2006, and the M.S. and Ph.D. degrees from Gyeongsang National University, Jinju, Republic of Korea, in 2008 and 2012, respectively. He is currently an Assistant Professor with the School of Mechanical Engineering and Electronic Information, China University of Geosciences, Wuhan, China.

His research interests include high-dimensional signal processing, orthogonal frequency division multiplexing, multiple-input multiple-output, and coding/decoding.